Inflamm. Res. (2012) 61:571–579
DOI 10.1007/s00011-012-0446-6

Inflammation Research

ORIGINAL RESEARCH PAPER

Metalloproteinases regulate CD40L shedding from platelets and pulmonary recruitment of neutrophils in abdominal sepsis

Milladur Rahman · Jonas Roller · Su Zhang · Ingvar Syk · Michael D. Menger · Bengt Jeppsson · Henrik Thorlacius

Received: 29 September 2011 / Accepted: 28 January 2012 / Published online: 21 February 2012

Abstract
Objective Platelets promote sepsis-induced activation of neutrophils via secretion of CD40L. However, the mechanism regulating the release of platelet-derived CD40L is not known. We hypothesized that matrix metalloproteinases (MMPs) might regulate shedding of platelet-expressed CD40L and neutrophil activation in sepsis.
Methods Wild-type C57BL/6 mice were subjected to cecal ligation and puncture (CLP). Animals were pretreated with a broad-range MMP inhibitor, GM6001, prior to CLP induction. Edema formation, CXC chemokine and myeloperoxidase (MPO) levels and bronchoalveolar neutrophils in the lung as well as plasma levels of CD40L were quantified. Flow cytometry was used to determine expression of Mac-1 on neutrophils and CD40L on platelets. Intravital fluorescence microscopy was used to analyze leukocyte–endothelial cell interactions in the pulmonary microcirculation.
Results The MMP inhibitor reduced sepsis-induced release of CD40L and maintained normal levels of CD40L on platelets. Inhibition of MMP decreased CLP-induced neutrophil expression of Mac-1, formation of CXC chemokines and edema as well as neutrophil infiltration in the lung. Intravital fluorescence microscopy revealed that the MMP inhibitor attenuated leukocyte adhesion in venules whereas capillary trapping of leukocytes was not affected by MMP inhibition.
Conclusions We describe a novel role of metalloproteinases in regulating platelet-dependent activation and infiltration of neutrophils in septic lung injury which might be related to controlling CD40L shedding from platelets. We conclude that targeting metalloproteinases may be a useful strategy for limiting acute lung injury in abdominal sepsis.

Keywords Adhesion · Neutrophils · Chemokines · Lung injury · Sepsis

Abbreviations

MMPs	Matrix metalloproteinases
CLP	Cecal ligation and puncture
BALF	Bronchoalveolar lavage fluid
i.v.	Intravenously
i.p.	Intraperitoneally
KC	Cytokine-induced neutrophil chemoattractant
MIP-2	Macrophage inflammatory protein-2
Mac-1	Membrane-activated complex-1
MNL	Monomorphonuclear leukocytes
MPO	Myeloperoxidase
PMNL	Polymorphonuclear leukocytes
IVM	Intravital microscopy

Introduction

Abdominal sepsis remains a major cause of mortality in intensive care units in spite of significant research efforts [1–3]. Management of patients with sepsis is largely limited to supportive therapies, which is partly due to an incomplete understanding of the underlying pathophysiology. Intestinal

Responsible Editor: Artur Bauhofer.

M. Rahman · J. Roller · S. Zhang · I. Syk · B. Jeppsson · H. Thorlacius (✉)
Department of Clinical Sciences, Malmo, Section of Surgery, Skåne University Hospital, Lund University, 205 02 Malmö, Sweden
e-mail: henrik.thorlacius@med.lu.se

J. Roller · M. D. Menger
Institute for Clinical and Experimental Surgery, University of Saarland, Homburg/Saar, Germany

perforation and contamination of the abdominal cavity with microbes and toxins stimulate local formation of numerous pro-inflammatory compounds, which subsequently diffuse into the systemic circulation [4, 5]. The lung is the most sensitive and clinically important end organ for the systemic inflammatory response in abdominal sepsis [6]. It is widely held that activation of neutrophils constitutes a central component in septic lung injury. For example, inhibition of neutrophil recruitment by targeting adhesion molecules, such as Mac-1 and LFA-1, effectively protects against pulmonary damage in sepsis [7]. CXC chemokines, including macrophage inflammatory protein-2 (MIP-2) and cytokine-induced neutrophil chemoattractant (KC), are primarily responsible for coordinating accumulation of neutrophils at sites of inflammation. However, the complex signaling cascades triggering neutrophil activation and recruitment in the lung initiated by a mixed bacterial flora and their released toxins are largely unknown [8, 9].

Platelets, beyond their classical role in thrombosis and hemostasis, exert numerous effects amplifying inflammatory responses and tissue injury. Recent data have demonstrated that platelets play an important role in abdominal sepsis [10] by releasing CD40L in the circulation, which, in turn, provokes up-regulation of Mac-1 and promotes pulmonary infiltration of neutrophils and tissue damage [11]. Indeed, a recent study demonstrated that plasma levels of soluble CD40L are markedly elevated in patients with sepsis [12]. In fact, most of the soluble CD40L in plasma is derived from platelets [11, 13]. However, the mechanisms regulating CD40L release from platelets are not known. Matrix metalloproteinases (MMPs) comprise a large family of more than 25 structurally and functionally related endopeptidases [14] with capacity to cleave the majority of matrix proteins as well as many non-matrix targets, such as chemokines, cytokines, adhesion molecules and surface receptors [15]. However, the role of MMPs in regulating cleavage of CD40L from platelets in abdominal sepsis remains elusive.

Based on the above, in this paper we hypothesized that MMPs may be involved in the regulation of shedding of platelet-expressed CD40L. More specifically, we evaluated the role of MMPs in controlling CD40L release from platelets and the subsequent activation and infiltration of neutrophils in the lung in polymicrobial sepsis. For this purpose, we used the CLP model of abdominal sepsis in mice.

Materials and methods

Animals

All experimental procedures were performed in accordance with the legislation on the protection of animals and were approved by the Regional Ethical Committee for Animal Experimentation at Lund University, Sweden. Wild-type male C57BL/6 (Jackson Laboratory, Bar Harbor, ME, USA) mice (20–25 g) were used in the experiments. Animals were anaesthetized by intraperitoneal (i.p.) administration of 75 mg ketamine hydrochloride (Hoffman-La Roche, Basel, Switzerland) and 25 mg xylazine (Janssen Pharmaceutica, Beerse, Belgium) per kg body weight.

Experimental model of sepsis

Polymicrobial sepsis was induced by cecal ligation and puncture (CLP) as previously described in detail [7]. In brief, mice were anesthetized and the abdomen was opened to exteriorize the cecum which was filled with feces by milking stool backwards from the ascending colon and a ligature was placed below the ileocecal valve. Cecum was then soaked in phosphate-buffered saline (PBS) (pH 7.4), punctured twice with a 21-gauge needle and returned into the peritoneal cavity. The abdominal wall was closed with a suture and mice were resuscitated with 1 ml of PBS subcutaneously. In order to delineate the role of MMPs, we used a potent, broad-spectrum hydroxamic acid inhibitor of MMPs, GM6001 (Galardin, N-[(2R)-2-(hydroxamidocarbonylmethyl)-4-methylpentanoyl]-L-tryptophan methylamide; Calbiochem, Darmstadt, Germany). GM6001 was given (40 mg/kg i.p.) 1 h before the CLP induction. Sham mice underwent the same surgical procedures, i.e., laparotomy and resuscitation, but the cecum was not ligated or punctured. The mice were then returned to their cages and provided food and water ad libitum. Animals were re-anesthetized at 6 and 24 h after CLP induction. The left lung was ligated and excised for edema quantification. From the right lung bronchoalveolar lavage fluid (BALF) was collected, in which the number of neutrophils was determined. Next, the lung was perfused with PBS and one part was fixed in formaldehyde for histology and the remaining lung tissue was weighed, snap-frozen in liquid nitrogen and stored at −80°C for later ELISA and myeloperoxidase (MPO) assays as described below.

Intravital fluorescence microscopy

In separate animals, a midline laparotomy was performed and extended to the side along the lower border of the right rib cage from the subxyphoidal to the midaxillary level. Under transient lowering of the stroke volume to 100 µl, the right diaphragm was incised to create a right-sided pneumothorax. The diaphragm was then stepwise coagulated and incised along the ventral chest wall to the midaxillary level. A parasternal thoracotomy was performed up to the level of the 4th intercostal space after coagulating the internal mammary and the intercostal

vessels. By this method, the main part of the right thorax wall could be averted to the side. During the preparation, great care was taken not to directly manipulate the lung tissue and the lung surface was intermittently rinsed with saline (37°C). A micromanipulator was used to fix a coverslip horizontally on the surface of the right lung. Horizontal movements of the lung tissue could be minimized by modulating a positive end-expiratory pressure between 5 and 7 cm H_2O and adjusting stroke volume (minimum 150 µl) and stroke frequency (minimum 100 strokes/min). Immediately after surgical preparation, the mice were put on the microscopic stage. Intravital fluorescence microscopy was performed after retrobulbar injection of 0.1 ml 0.1% rhodamine 6G (Sigma-Aldrich, Taufkirchen, Germany) for direct staining of white blood cells and 0.1 mL 5% FITC-dextran (MW 150 000, contrast enhancement; Sigma Chemical Co., St. Louis, MO, USA). The subpleural pulmonary microvasculature was visualized by means of a modified Olympus microscope (BX50WI, Olympus Optical Co. GmbH, Hamburg, Germany) equipped with a 100 W mercury lamp and filter sets for blue (450−490 nm excitation and >520 nm emission wavelength) and green (530−560 nm excitation and >580 nm emission wavelength) light epi-illumination. Microscopic images were televised by means of a charge-coupled device video camera and recorded digitally. By means of a 20× objective (NA 0.4) a magnification of ×990 was achieved. With this setup, all parts of the subpleural pulmonary microvasculature, i.e. arterioles, venules and capillaries, could be identified. For the measurement of 3−5 venules and capillaries, Regions of Interest (ROIs) were selected randomly in each animal. Leukocyte rolling was determined by counting the number of such cells passing a reference point in the venule per 20 s. Firm adhesion was measured by counting the number of cells adhering to the venular endothelium and remaining stationary for 20 s.

Systemic leukocyte and platelet counts

Blood was collected from the tail vein and mixed with Turk's solution (0.2 mg gentian violet in 1 ml glacial acetic acid, 6.25% v/v) in a 1:20 dilution for quantification of polymorphonuclear leukocytes (PMNL) and monomorphonuclear leukocytes (MNL) or with Stromatol solution (Mascia Brunelli SpA, Viale Monza, Milan, Italy) in a dilution of 1:50 for identification of platelets in a Burker chamber.

Lung edema

The left lung was excised, washed in PBS, gently dried using blotting paper and weighed. The tissue was then dried at 60°C for 72 h and re-weighed. The change in the ratio of wet weight to dry weight was used as an indicator of lung edema formation.

Bronchoalveolar lavage fluid

Bronchoalveolar lavage fluid was collected by washing five times with 1 ml of PBS containing 5 mM EDTA and was then centrifuged; numbers of MNLs and PMNLs were counted in a Burker chamber.

MPO activity

MPO in the lung tissue was assayed as described by Asaduzamman et al. [7]. Briefly, frozen tissue was thawed and homogenized in 1 ml of 0.5% hexadecyltrimethylammonium bromide. Next, the sample was freeze-thawed, after which the MPO activity of the supernatant was measured. The enzyme activity was determined spectrophotometrically as the MPO-catalyzed change in absorbance in the redox reaction of H_2O_2 (450 nm, with a reference filter 540 nm, 25°C). Values were expressed as MPO units per gram tissue.

ELISA

Plasma levels of CD40L and lung homogenate levels of MIP-2 and KC were analyzed 6 h and 24 h after CLP, respectively, by using commercially available ELISA kits (R&D Systems). For soluble CD40L analysis, plasma was collected on ice using citrate as anticoagulant and centrifuged for 20 min at 2,000*g* immediately after collection. An additional centrifugation at 10,000*g* for 10 min at 4°C was employed for complete removal of platelets and stored at −20°C for further use. Plasma samples were then diluted with a sterile buffer (10% fetal calf serum in PBS, pH 7.4) and analyzed using the protocols provided.

Flow cytometry

For analysis of surface CD40L expression on platelets and Mac-1 expression on circulating neutrophils, blood was collected into syringes containing 1:10 acid citrate dextrose at 6 h post CLP induction. Immediately after collection, blood samples were incubated with an anti-CD16/CD32 antibody blocking FcγIII/II receptors in order to reduce non-specific labeling for 10 min at room temperature (RT), and then incubated with PE-conjugated anti-Gr-1 (clone RB6-8C5, rat IgG2b), and APC-conjugated anti-Mac-1 (clone M1/70, integrin α_M chain, rat IgG2b) antibodies. Another set of samples were stained with FITC-conjugated anti-CD41 (clone MWReg30, integrin α_{IIb} chain, rat IgG1) and PE-conjugated anti-CD40L (clone MR1, hamster IgG,

eBioscience, San Diego, CA, USA) antibodies (all antibodies except where indicated were purchased from BD Biosciences Pharmingen, San Jose, CA, USA). Cells were fixed with 1% formaldehyde solution; erythrocytes were lysed using FACS lysing solution (BD Biosciences Pharmingen) and then neutrophils and platelets were recovered following centrifugation. Flow-cytometric analysis was performed according to standard settings on a FACScalibur flow cytometer (Becton–Dickinson, Mountain View, CA, USA) and a viable gate was used to exclude dead and fragmented cells.

Histology

Lungs samples were fixed in 4% formaldehyde phosphate buffer overnight and then dehydrated and paraffin-embedded. Six-μm sections were stained with hematoxylin and eosin (H&E).

Statistics

Data are presented as mean values ± standard error of the means (SEM). Statistical evaluations were performed using Kruskal–Wallis one-way analysis of variance on ranks followed by multiple comparisons versus control group (Dunnett's method). $P < 0.05$ was considered significant and n represents the number of animals in each group.

Results

MMPs regulate platelet shedding of CD40L

CLP increased plasma levels of CD40L by more than 2.5-fold, from 71 ± 6 pg/ml in the sham animals to 209 ± 23 pg/ml (Fig. 1a; $P < 0.05$ vs. Sham, $n = 5$). In parallel, surface expression of CD40L on platelets decreased; mean fluorescent intensity (MFI) was 50 ± 4 in sham and 29± in septic mice (Fig. 1b; $P < 0.05$, $n = 5$). Administration of GM6001, a broad-spectrum MMP inhibitor, reduced CLP-induced plasma levels of CD40L by more than 87% (Fig. 1a; $P < 0.05$ vs. Vehicle + CLP, $n = 5$). Concomitantly, inhibition of MMP activity completely blocked the CLP-induced reduction of surface CD40L on platelets (Fig. 1b, c; $P < 0.05$ vs. Vehicle + CLP, $n = 5$). Moreover, CLP caused a significant reduction in the systemic number of platelets after 24 h, which was reversed to normal levels by pretreatment with GM6001 (Table 1).

MMPs regulate Mac-1 expression on neutrophils

Induction of CLP increased surface expression of Mac-1 on neutrophils (Fig. 2a). MFI values of Mac-1 were 734 ± 22 in Sham and 1402 ± 74 in septic mice (Fig. 2b; $P < 0.05$ vs. Sham, $n = 5$). This indicates circulating neutrophils are indeed activated in this model of sepsis. Administration of GM6001 greatly decreased neutrophil up-regulation of

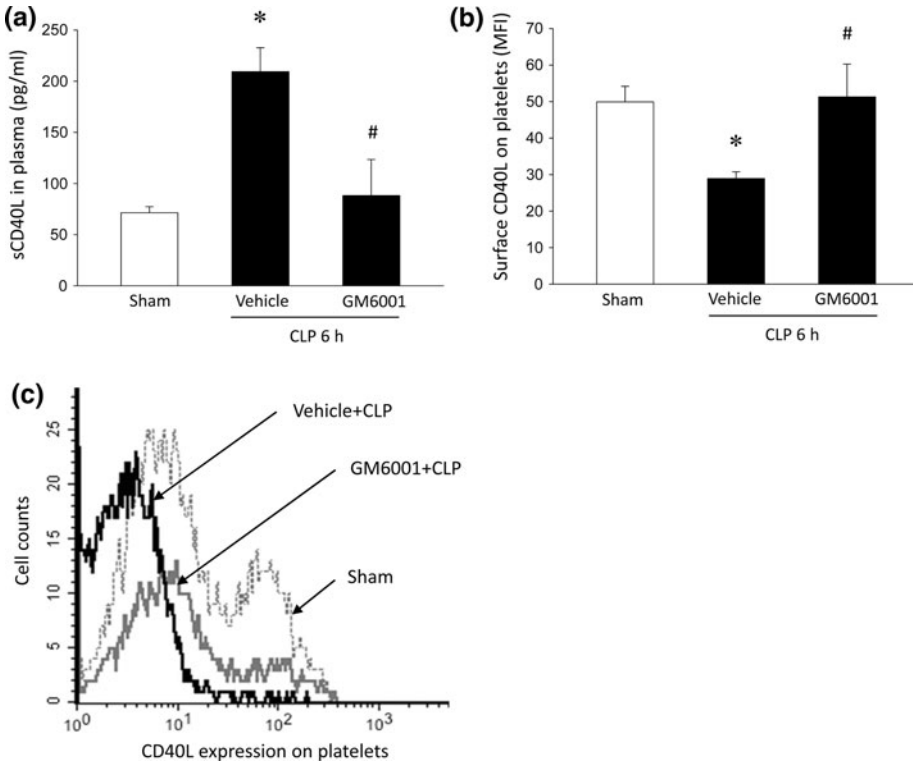

Fig. 1 MMPs regulate CLP-induced shedding of CD40L from platelets. Plasma levels of soluble CD40L (**a**), surface expression of CD40L on platelets (**b**) and a representative histogram (**c**) 6 h after CLP. Animals were treated with vehicle or the MMP inhibitor GM6001 prior to CLP induction. Sham-operated animals served as negative controls. Data represents mean ± SEM and $n = 5$. $^{*}P < 0.05$ versus Sham and $^{\#}P < 0.05$ versus Vehicle + CLP

Mac-1 in CLP mice (Fig. 2a). In fact, MFI values of Mac-1 on neutrophils decreased from 1402 ± 74 down to 963 ± 83 in CLP mice pretreated with the MMP inhibitor, corresponding to a 65% reduction (Fig. 2b; $P < 0.05$ vs. Vehicle + CLP, $n = 5$).

Table 1 Systemic platelet and leukocyte differential counts

	Platelets	MNLs	PMNLs	Total leukocytes
Sham	681 ± 53	5.2 ± 0.3	1.7 ± 0.3	6.9 ± 0.6
Vehicle + CLP	458 ± 15[a]	1.1 ± 0.1[a]	0.7 ± 0.1[a]	1.8 ± 0.2[a]
GM6001 + CLP	694 ± 14[b]	1.4 ± 0.4	0.8 ± 0.1	2.2 ± 0.5

Blood was collected from sham-, vehicle- and GM6001-treated mice subjected to cecal ligation and puncture (CLP) for 24 h. Cells were identified as platelets, monomorphonuclear leukocytes (MNLs) and polymorphonuclear leukocytes (PMNLs). Data represents mean ± SEM, 10^6 cells/ml and $n = 5$–6

[a] $P < 0.05$ versus Sham

[b] $P < 0.05$ versus Vehicle + CLP

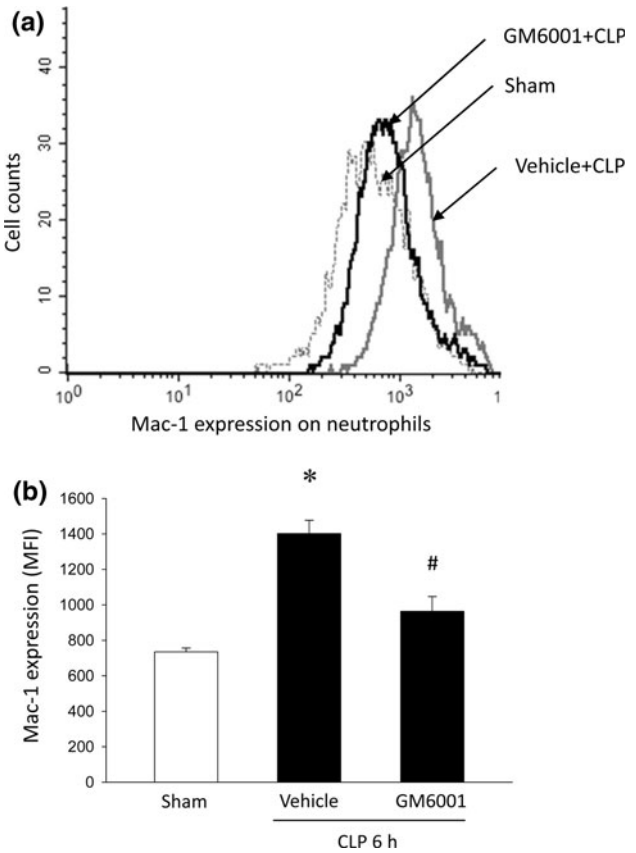

Fig. 2 MMPs regulate CLP-induced expression of Mac-1 on neutrophils. Mac-1 expression on neutrophils (Gr-1$^+$ cells) 6 h after induction of CLP. A representative histogram (**a**) and aggregate data (**b**) of Mac-1 expression on neutrophils. Animals were treated with vehicle or the MMP inhibitor (GM6001) prior to CLP induction. Sham-operated animals served as negative controls. Data are representative of four other experiments ($n = 5$)

MMPs regulate neutrophil recruitment in the lung

Pulmonary accumulation of neutrophils was quantified by analyzing levels of myeloperoxidase (MPO), an indicator of neutrophils, in the lung. CLP increased MPO levels in the lung by more than 12-fold (Fig. 3a; $P < 0.05$ vs. Sham, $n = 5$). Administration of GM6001 decreased MPO activity in the lung by more than 56% in septic mice (Fig. 3a; $P < 0.05$ vs. Vehicle + CLP, $n = 5$). Moreover, cellular analysis of BALF showed that the number of neutrophils in the bronchoalveolar space increased by 13-fold 24 h after induction of CLP (Fig. 3b; $P < 0.05$ vs. Sham, $n = 5$). Notably, inhibition of MMP activity reduced CLP-induced recruitment of neutrophils into the bronchoalveolar compartment from 143 ± 17 × 10^3 down to 50 ± 12 × 10^3 cells, corresponding to a 70% reduction in neutrophil accumulation (Fig. 3b; $P < 0.05$ vs. Vehicle + CLP, $n = 5$). CLP induction in mice provoked a clear-cut leukocytopenia at 24 h. Administration of GM6001 had no effect on the levels of circulating leukocytes in CLP mice (Table 1).

MMPs regulate CXC chemokine formation in the lung

CXC chemokines, such as MIP-2 and KC, are known to regulate neutrophil trafficking in the lung. Levels of MIP-2 and KC were low but detectable in sham animals (Fig. 3d). We observed that production of CXC chemokines in the lung was markedly increased in CLP mice (Fig. 3d; $P < 0.05$ vs. Sham, $n = 5$–6). Interestingly, it was found that pretreatment with GM6001 reduced CLP-induced formation of MIP-2 and KC in the lung by more than 43 and 64%, respectively (Fig. 3d; $P < 0.05$ vs. Vehicle + CLP, $n = 5$–6).

Inhibition of MMPs protects against septic lung injury

CLP caused significant pulmonary damage, characterized by a prominent enhancement in lung edema formation: wet:dry ratio increased from 4.5 ± 0.1 to 5.4 ± 0.1 (Fig. 3c; $P < 0.05$ vs. Sham, $n = 5$). Note that baseline values of wet:dry ratio in sham mice represent normal levels in healthy animals and only an increase in wet:dry ratio represents actual edema formation. Administration of GM6001 decreased CLP-induced lung wet:dry ratio from 5.4 ± 0.1 to 4.4 ± 0.1, corresponding to 95% reduction in lung edema (Fig. 3c; $P < 0.05$ vs. Vehicle + CLP, $n = 5$). Moreover, morphologic examination revealed normal microarchitecture in lungs of sham-operated animals (Fig. 4a), whereas CLP caused severe destruction of the

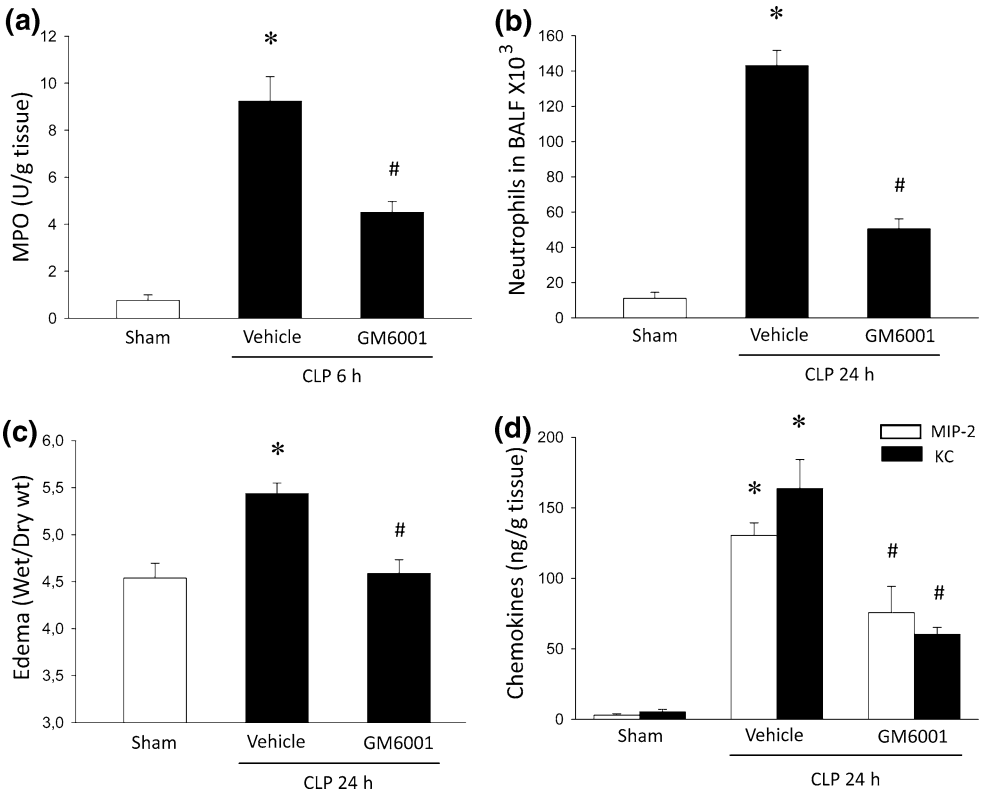

Fig. 3 MMPs regulate CLP-induced pulmonary inflammation. Lung MPO (**a**) levels 6 h after CLP, number of BALF neutrophils (**b**), edema formation (**c**) and pulmonary levels of CXC chemokines (MIP-2 and KC) (**d**) 24 h after CLP induction. Animals were treated with vehicle or the MMP inhibitor GM6001 prior to CLP induction. Sham-operated animals served as negative controls. Data represents mean ± SEM and $n = 5$–6. $^{*}P < 0.05$ versus Sham and $^{\#}P < 0.05$ versus Vehicle+CLP

pulmonary tissue structure characterized by extensive edema of the interstitial tissue and massive infiltration of neutrophils (Fig. 4b). Pretreatment with GM6001 markedly reduced CLP-induced destruction of the tissue architecture and reduced neutrophil infiltration in the lung (Fig. 4c).

MMPs regulate leukocyte adhesion in the lung microvasculature

In order to study the detailed influence of MMPs on sepsis-induced leukocyte–endothelial cell interactions in the pulmonary microcirculation, we adopted intravital fluorescence microscopy. It was found that CLP triggered a clear-cut increase in leukocyte adhesion in capillaries and venules of the pulmonary microvasculature (Fig. 5a, e). Inhibition of MMP activity decreased CLP-induced leukocyte adhesion in venules by 64% (Fig. 5b, d; $P < 0.05$ vs. Vehicle + CLP, $n = 5$) but had no effect on capillary sticking of leukocytes (Fig. 5f, g). Administration of GM6001 had no impact on leukocyte rolling in the lung microcirculation of septic animals (Fig. 5c).

Discussion

Our data show that MMPs regulate sepsis-induced lung injury via promotion of neutrophil recruitment to the lung. We found that MMPs reduce CD40L shedding from platelets and up-regulation of Mac-1 on neutrophils as well as formation of CXC chemokines in the lung. Thus, this study demonstrates that MMPs are involved in the regulation of platelet shedding of CD40L and activation of neutrophils in septic lung damage and may be a useful target in abdominal sepsis.

Emerging data show that platelets are not only essential for homeostasis, thrombosis, and wound healing, but also play an important role in inflammation and tissue injury. We have recently demonstrated that platelets constitute a critical component in polymicrobial sepsis by activating and supporting neutrophil recruitment to the lung [10]. This platelet-dependent activation of neutrophils and subsequent lung damage has recently been shown to be mediated by CD40L released from platelets in abdominal sepsis [11]. In this context, it is also interesting to note that clinical studies have shown that plasma levels of CD40L in the plasma are elevated in patients with sepsis [12, 16]. However, the mechanisms regulating sepsis-induced platelet shedding of CD40L are not known. We focused here on the role of MMPs and found that administration of a MMP inhibitor reduced soluble levels of CD40L and concomitantly increased expression of CD40L on the surface of platelets in septic mice, suggesting that platelet shedding of CD40L is controlled by MMPs in polymicrobial sepsis. This study is the first to show that MMPs can regulate platelet

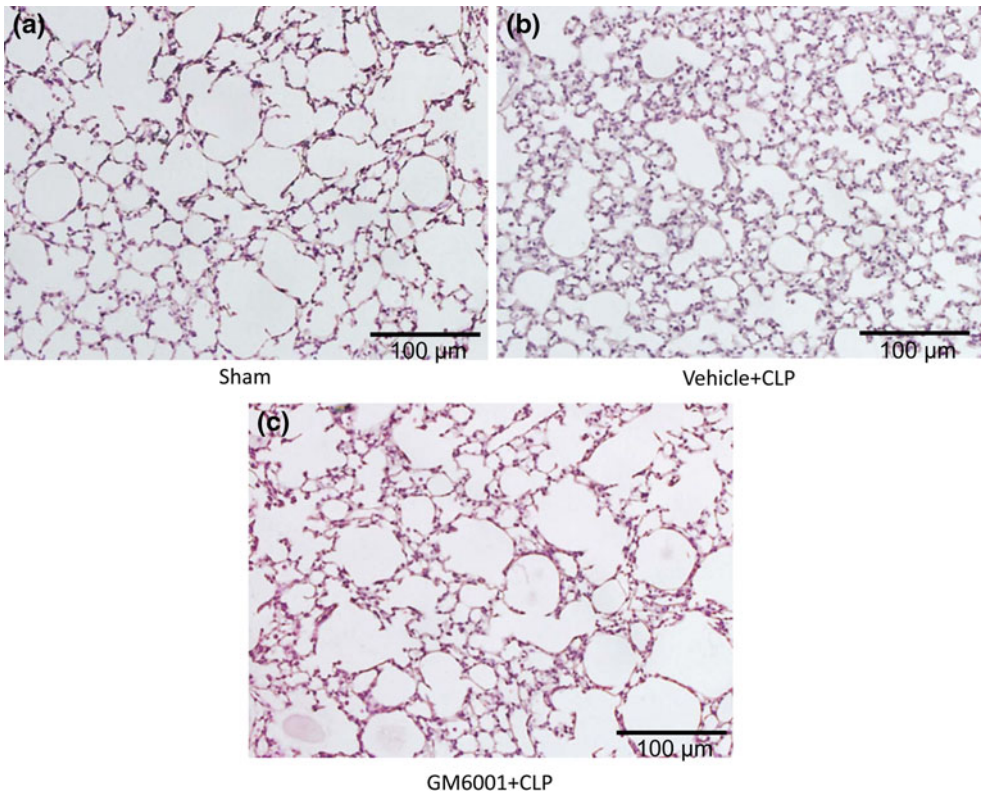

Fig. 4 MMPs regulate CLP-induced lung damage. Representative hematoxylin and eosin-stained sections of lung tissue. Sham-operated animals served as negative controls (**a**). Animals were treated with vehicle (**b**) or the MMP inhibitor GM6001 (**c**) prior to CLP induction and samples were harvested 24 h later ($n = 5$). *Scale bar* indicates 100 μm

functions in sepsis. In this context, it should be noted that one weakness with the present study is that we did not study the effect of MMP inhibition on survival.

It is widely held that neutrophil recruitment causing tissue injury and disturbed gaseous exchange is a rate-limiting step in septic lung injury [7, 17]. In this study, it was observed that inhibition of MMPs reduced pulmonary infiltration of neutrophils. Additionally, we observed that MMP inhibition not only reduced neutrophil recruitment but also decreased sepsis-induced edema formation and tissue destruction in the lung, suggesting that targeting MMPs may protect against pulmonary damage in abdominal sepsis. This notion is in line with most studies on MMP inhibition in models of endotoxemia and severe infections [18–20], although some exceptions have been reported. Indeed, ample data show that mice challenged by different bacteria or bacterial toxins, different doses of bacteria and toxins and routes of administration display different phenotypes. Indeed, injection of single-bacteria toxins may not represent the pathophysiology of clinical sepsis very well. In contrast, the CLP model, in which the intestine is punctured and the bowel contents are allowed to contaminate the abdominal cavity, seems to be more reminiscent of the events and course in polymicrobial sepsis in terms of cytokine responses and vascular and metabolic changes [21, 22]. To study the detailed impact of MMPs on leukocyte–endothelium interactions, we used intravital fluorescence microscopy of the lung microcirculation. We were able to demonstrate that MMP inhibition decreased sepsis-induced leukocyte adhesion in venules but not capillary trapping of leukocytes. Considering that venular adhesion of leukocytes is mediated by specific adhesion molecules and that trapping of leukocytes in capillaries is dependent on size restrictions in the capillary lumen due to increased stiffness of leukocytes [23–26], our data suggest that MMPs mainly regulate the adhesion molecule-dependent accumulation of leukocytes in the lung. This notion is also supported by the observation here that inhibition of MMPs decreased neutrophil expression of Mac-1, which is known to mediate pulmonary recruitment of neutrophils in abdominal sepsis [7]. We have previously shown that neutrophil expression of Mac-1 is dependent on platelet-derived CD40L in polymicrobial sepsis [11]. As mentioned above, MMPs also abolished sepsis-triggered platelet shedding of CD40L underling the importance of the CD40L–Mac-1 axis in abdominal sepsis. Tissue navigation of neutrophils is coordinated by secreted CXC chemokines [27]. In the present study, we observed that MMP inhibition attenuated sepsis-induced formation of MIP-2 and KC in the lung, which may also contribute to the protective

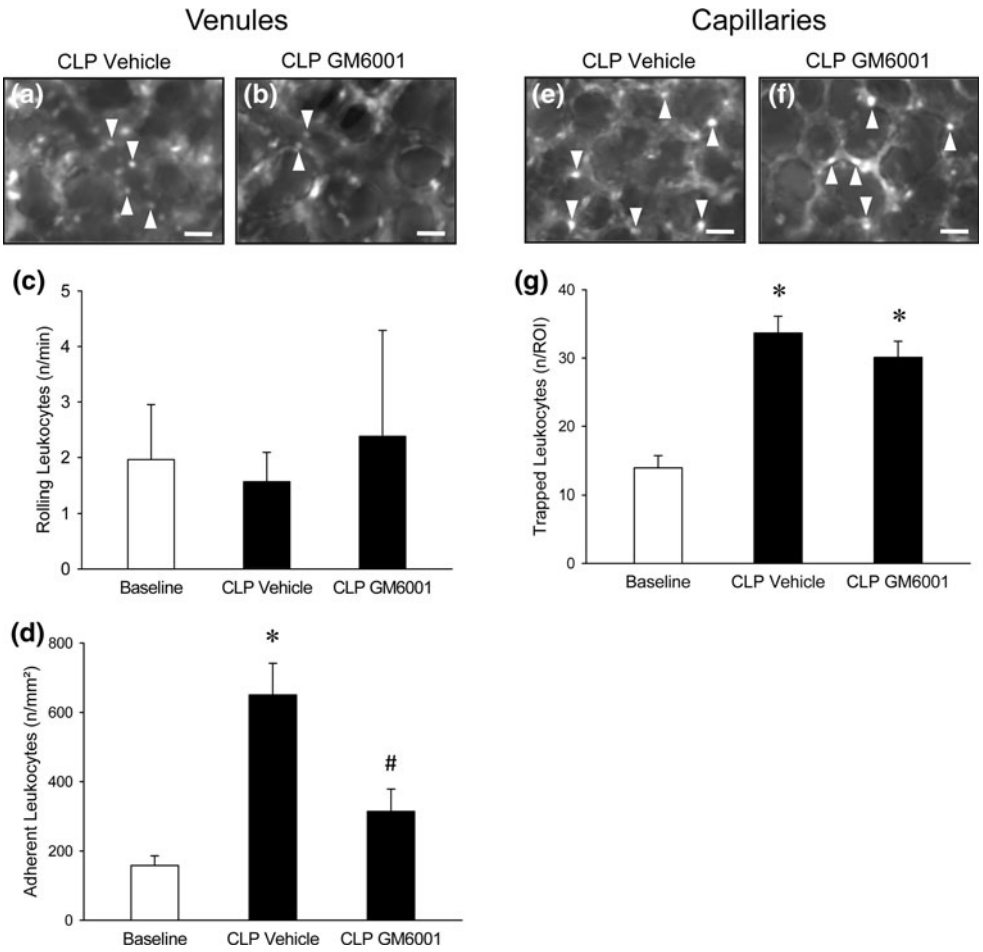

Fig. 5 MMPs regulate CLP-induced leukocyte adhesion in the lung microvasculature. Intravital fluorescence microscopy was used to study leukocyte–endothelium interactions in the pulmonary microcirculation 6 h after CLP induction as described in : "Materials and methods". Leukocyte rolling and adhesion in venules (**a**–**d**). The number of trapped leukocytes was determined in capillaries (**e**–**g**). Animals were treated with vehicle or the MMP inhibitor GM6001 prior to CLP induction. Sham-operated animals served as negative (baseline) controls. Data represents mean ± SEM and $n = 5$. $^{*}P < 0.05$ versus Sham and $^{\#}P < 0.05$ versus Vehicle + CLP

effect of MMP inhibition in septic lung damage. The mechanism by which MMPs control CXC chemokine formation in the lung is not known at present. However, numerous studies have shown that MMPs can promote Toll-like receptor (TLR)-4 activation on macrophages by generating several different TLR4 ligands, such as soluble CD14 [28], which, in turn, can trigger generation of CXC chemokines. Thus, MMPs' functions in sepsis are not limited to the regulation of the CD40L–Mac-1 axis but are most likely operating at multiple concomitant levels to promote neutrophil accumulation at sites of inflammation.

Taken together, our results demonstrate that inhibition of MMPs reduced platelet shedding of CD40L, Mac-1 up-regulation on neutrophils and CXC chemokine formation in the lung, although the relative importance of these parameters in mediating neutrophil-dependent lung injury remains elusive. Moreover, we found that blocking MMPs not only decreased pulmonary infiltration of neutrophils but also reduced lung damage in septic animals. Thus, based on our results, we suggest that MMPs may be a useful target for inhibiting lung damage in abdominal sepsis.

Acknowledgments This work was supported by grants from the Swedish Medical Research Council (2009-4872), Crafoordska stiftelsen, Einar och Inga Nilssons stiftelse, Harald och Greta Jaenssons stiftelse, Greta och Johan Kocks stiftelser, Fröken Agnes Nilssons stiftelse, Franke och Margareta Bergqvists stiftelse för främjande av cancerforskning, Magnus Bergvalls stiftelse, Mossfelts stiftelse, Nanna Svartz stiftelse, Ruth och Richard Julins stiftelse, Svenska Läkaresällskapet, Allmäna sjukhusets i Malmö stiftelse för bekämpande av cancer, MAS fonder, Malmö University Hospital and Lund University.

References

1. Cohen J. The immunopathogenesis of sepsis. Nature. 2002;420:885–91.
2. Heyland DK, Hopman W, Coo H, Tranmer J, McColl MA. Long-term health-related quality of life in survivors of sepsis. Short Form 36: a valid and reliable measure of health-related quality of life. Crit Care Med. 2000;28:3599–605.
3. Martin GS, Mannino DM, Eaton S, Moss M. The epidemiology of sepsis in the United States from 1979 through 2000. N Engl J Med. 2003;348:1546–54.
4. Gorbach SL, Bartlett JG. Anaerobic infections. 1. N Engl J Med. 1974;290:1177–84.
5. Simon GL, Gorbach SL. Intestinal flora in health and disease. Gastroenterology. 1984;86:174–93.

6. Babayigit H, Kucuk C, Sozuer E, Yazici C, Kose K, Akgun H. Protective effect of beta-glucan on lung injury after cecal ligation and puncture in rats. Intensive Care Med. 2005;31:865–70.
7. Asaduzzaman M, Zhang S, Lavasani S, Wang Y, Thorlacius H. LFA-1 and MAC-1 mediate pulmonary recruitment of neutrophils and tissue damage in abdominal sepsis. Shock. 2008;30:254–9.
8. Parrillo JE. Mechanisms of disease—pathogenetic mechanisms of septic shock. N Engl J Med. 1993;328:1471–7.
9. Remick DG. Pathophysiology of sepsis. Am J Pathol. 2007;170: 1435–44.
10. Asaduzzaman M, Lavasani S, Rahman M, Zhang S, Braun OO, Jeppsson B, et al. Platelets support pulmonary recruitment of neutrophils in abdominal sepsis. Crit Care Med. 2009;37:1389–96.
11. Rahman M, Zhang S, Chew M, Ersson A, Jeppsson B, Thorlacius H. Platelet-derived CD40L (CD154) mediates neutrophil upregulation of Mac-1 and recruitment in septic lung injury. Ann Surg. 2009;250:783–90.
12. Chew M, Rahman M, Ihrman L, Erson A, Zhang S, Thorlacius H. Soluble CD40L (CD154) is increased in patients with shock. Inflamm Res. 2010;59:979–82.
13. Henn V, Steinbach S, Buchner K, Presek P, Kroczek RA. The inflammatory action of CD40 ligand (CD154) expressed on activated human platelets is temporally limited by coexpressed CD40. Blood. 2001;98:1047–54.
14. Ra HJ, Parks WC. Control of matrix metalloproteinase catalytic activity. Matrix Biol. 2007;26:587–96.
15. Stamenkovic I. Extracellular matrix remodelling: the role of matrix metalloproteinases. J Pathol. 2003;200:448–64.
16. Inwald DP, Faust SN, Lister P, Peters MJ, Levin M, Heyderman R, et al. Platelet and soluble CD40L in meningococcal sepsis. Intensive Care Med. 2006;32:1432–7.
17. Czermak BJ, Breckwoldt M, Ravage ZB, Huber-Lang M, Schmal H, Bless NM, et al. Mechanisms of enhanced lung injury during sepsis. Am J Pathol. 1999;154:1057–65.
18. Cena JJ, Lalu MM, Cho WJ, Chow AK, Bagdan ML, Daniel EE, et al. Inhibition of matrix metalloproteinase activity in vivo protects against vascular hyporeactivity in endotoxemia. Am J Physiol Heart Circ Physiol 298:H45–H51.
19. Maitra SR, Bhaduri S, Valane PD, Tervahartiala T, Sorsa T, Ramamurthy N. Inhibition of matrix metalloproteinases by chemically modified tetracyclines in sepsis. Shock. 2003;20: 280–5.
20. Steinberg J, Halter J, Schiller HJ, Dasilva M, Landas S, Gatto LA, et al. Metalloproteinase inhibition reduces lung injury and improves survival after cecal ligation and puncture in rats. J Surg Res. 2003;111:185–95.
21. Remick DG, Newcomb DE, Bolgos GL, Call DR. Comparison of the mortality and inflammatory response of two models of sepsis: lipopolysaccharide vs. cecal ligation and puncture. Shock. 2000;13:110–6.
22. Wichterman KA, Baue AE, Chaudry IH. Sepsis and septic shock–a review of laboratory models and a proposal. J Surg Res. 1980;29:189–201.
23. Downey GP, Worthen GS, Henson PM, Hyde DM. Neutrophil sequestration and migration in localized pulmonary inflammation. Capillary localization and migration across the interalveolar septum. Am Rev Respir Dis. 1993;147:168–76.
24. Nolte D, Kuebler WM, Muller WA, Wolff KD, Messmer K. Attenuation of leukocyte sequestration by selective blockade of PECAM-1 or VCAM-1 in murine endotoxemia. Eur Surg Res. 2004;36:331–7.
25. Sikora L, Johansson AC, Rao SP, Hughes GK, Broide DH, Sriramarao P. A murine model to study leukocyte rolling and intravascular trafficking in lung microvessels. Am J Pathol. 2003;162:2019–28.
26. Yoshida K, Kondo R, Wang Q, Doerschuk CM. Neutrophil cytoskeletal rearrangements during capillary sequestration in bacterial pneumonia in rats. Am J Respir Crit Care Med. 2006;174:689–98.
27. Schramm R, Thorlacius H. Staphylococcal enterotoxin B-induced acute inflammation is inhibited by dexamethasone: important role of CXC chemokines KC and macrophage inflammatory protein 2. Infect Immun. 2003;71:2542–7.
28. Senft AP, Korfhagen TR, Whitsett JA, Shapiro SD, LeVine AM. Surfactant protein-D regulates soluble CD14 through matrix metalloproteinase-12. J Immunol. 2005;174:4953–9.